Metastable chaos in the ammonia ring laser

R. Dykstra, J. T. Malos, and N. R. Heckenberg

Physics Department, University of Queensland, Queensland, 4072, Australia

R. G. McDuff

Advanced Computational Modelling Centre, University of Queensland, Queensland 4072, Australia

We report experimental studies of metastable chaos in the far-infrared ammonia ring laser. When the laser pump power is switched from above chaos threshold to slightly below, chaotic intensity pulsations continue for a varying time afterward before decaying to either periodic or cw emission. The behavior is in good qualitative agreement with that predicted by the Lorenz equations, previously used to describe this laser. The statistical distribution of the duration of the chaotic transient is measured and shown to be in excellent agreement with the Lorenz equations in showing a modified exponential distribution. We also give a brief numerical analysis and graphical visualization of the Lorenz equations in phase space illustrating the boundary between the metastable chaotic and the stable fixed point basins of attraction. This provides an intuitive understanding of the metastable dynamics of the Lorenz equations and the experimental system. [S1050-2947(97)00610-0]

PACS number(s): 42.65.Sf, 47.52.+j, 42.55.−f, 42.60.Mi

I. INTRODUCTION

Deterministic chaos has been demonstrated in many experimental systems, one well known one being the system devised by Weiss and Brock [1]. In this system the output of a far-infrared ring laser produces chaotic time series which are well described by the Lorenz-Haken laser equations [2], which are isomorphic to the celebrated Lorenz equations derived from the equations of convective fluid flow [3]. This system has afforded a number of direct experimental observations of chaotic behavior that have been in excellent qualitative agreement, at the very least, with the dynamics calculated from the Lorenz equations. In this work, the system used is very similar to that of [1] and has also demonstrated semiquantitative agreement with calculation [4–6].

If the value of a parameter is changed, transient behavior can ensue before the system settles to a new long-term behavior characteristic of the new parameter value. When the new state is not far below the chaos threshold, metastable chaos, i.e., a burst of transient chaotic behavior, can be observed [7–9]. In this metastable regime, the duration of the chaotic transient has been shown to depend sensitively upon the initial conditions chosen and gives an exponential distribution of metastable duration times for randomly chosen initial conditions [7]. The mean of the distribution, effectively the average metastable duration time, has also been shown to vary exponentially with the pump parameter wherein the exponent is referred to as the ''critical exponent'' for the metastable behavior [10–12].

This work investigates such metastable phenomena in the ammonia laser [4–6]. We allow the system to evolve for a time in the chaotic regime and then quickly switch the laser pump power to a value slightly below the threshold value for chaos. Metastable chaotic transients are subsequently observed which are shown to be in excellent qualitative agreement with corresponding transients calculated from the Lorenz equations. By repetitively switching the pump power from above to below the chaos threshold, the chaotic nature

of the laser output together with system noise provides a sufficiently random selection of initial conditions to demonstrate the statistical distribution of the duration of the transients and allows comparison with theory. Once again, excellent agreement is shown. Furthermore, the mean of the experimental distribution is shown to vary with pump parameter in a manner consistent with that of the Lorenz equations. As defined by [10], an experimental critical exponent of the system is determined and compared with exponents obtained from the Lorenz equations.

However, the exponential distribution of the duration times for metastable transients breaks down for transients consisting of two, one, or zero chaotic pulses. There is a much larger number of these short or zero duration transients than predicted by an exponential distribution. This is observed both in the laser and in the solutions to the equations. To investigate this we provide a numerical visualization of the phase space for the three variables of the Lorenz equations. This graphically illustrates the geometrical form of the basin of attraction of the metastable behavior and also the boundary between this and the basin for short or zero duration transients. The visualization gives an intuitive explanation as to why the distribution of the duration times for metastable transients yields a much larger proportion of very short transients.

II. EXPERIMENTAL SYSTEM AND THE LORENZ MODEL

The system used (Fig. 1) is essentially the same as used in previous studies of chaotic and transient behavior of the ammonia laser [4–6]. A $^{13}CO_2$ laser optically pumps a $^{15}NH_3$ far-infrared (FIR) ring laser and the pump power can be rapidly switched using the transmitted beam from an acousto-optic modulator. The form of the pump power with time (from the diffracted beam) is observed using a HgCdTe detector and the output emission of the FIR laser is detected using a Schottky barrier diode detector. The ring laser output
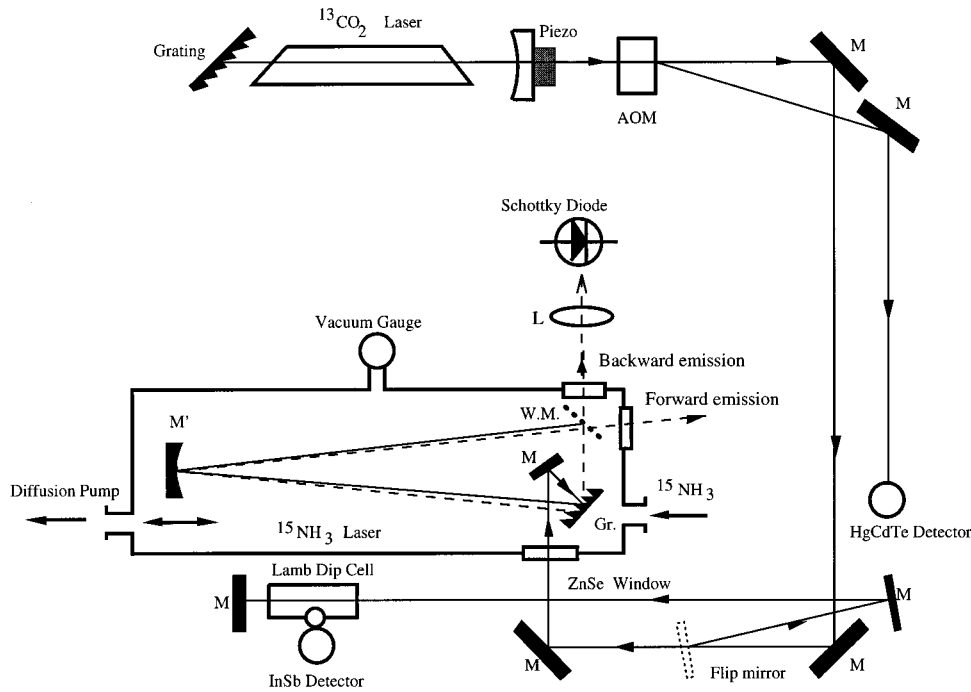
FIG. 1. Experimental setup. M' is a 2.0 m R.O.C. movable mirror to control the ring laser tuning. Gr. is grating to couple the CO_2 radiation into the ring resonator (80 lines per mm). W.M. is the wire mesh output coupler (5 lines per mm). See text for details.

is coupled via a wire mesh and the backward traveling wave (with respect to pump beam direction) is monitored through a port. Pump radiation is coupled into the ring via a ruled grating with rule spacing designed to specularly reflect the FIR radiation. The frequency of the pump laser is tuned via a piezo mounted mirror and is monitored using a Lamb Dip cell. The ring laser is tuned mechanically via a translatable curved mirror. The ammonia pressure used throughout the experiments was 38 μbar. Pump laser power was typically between 5.0 and 6.5 W.

The equations used to describe the system are the Lorenz equations [3]:

$$\dot{x} = \sigma(y-x),$$

$$\dot{y} = x(r-z)-y, \qquad (2.1)$$

$$\dot{z} = xy - bz.$$

The variables x,y,z, correspond to the laser electric field E and the polarization P and inversion D of the lasing medium, respectively, according to the isomorphism demonstrated by Haken [2]. The parameters σ and b depend on the relaxation rates of the laser variables. The pump power is the control parameter for the system and represented by r. Although there has been considerable controversy concerning the validity of this model to describe the laser system (outlined in [5]), the final qualitative agreement with experimental observations in this work continues to be exceptional.

The regions of particular dynamic behavior (e.g., chaotic, metastable, periodic, steady state) as a function of r are illustrated in Fig. 2 and are described briefly as follows. $r=1$ corresponds to the threshold for lasing and so for r less than 1, the origin is stable and there is no lasing. For r between 1 and r_{ch} [where $r_{ch} = \sigma(\sigma+b+3)/(\sigma-b-1)$ is the threshold

for chaos] the origin is unstable and there are instead two stable fixed point solutions $(\pm\sqrt{b(r-1)}, \pm\sqrt{b(r-1)}, r-1)$ corresponding to steady cw operation. Between $r=1$ and r_{ch} there are two further significant values, r_0 and r_1, that are relevant to defining the metastable chaotic regime, with $1 < r_0 < r_1 < r_{ch}$ [7]. For r between 1 and r_0, the basins of attraction of each of the fixed points make up all of phase space defined by x,y,z and hence all points evolve to either one of the fixed points. For r between r_0 and r_1, there is now a region of metastable chaos. Initial conditions chosen within this region behave chaotically but eventually end up on the fixed points. Initial conditions chosen outside the metastable region also evolve to the fixed points but do not have an initial chaotic transient. There are therefore still two basins of attraction each belonging to the two fixed points since all initial conditions eventually evolve to these points. For r between r_1 and r_{ch}, however, there are three basins of attraction (two fixed stable points and the one which displays complex dynamics). All trajectories in each basin of attraction remain there. Initial conditions chosen in either of the fixed points' basins of attraction evolve to the respective fixed point and initial conditions chosen in the chaotic attractor's basin of attraction continue to evolve chaotically indefinitely. In this work, we investigate the behavior for which
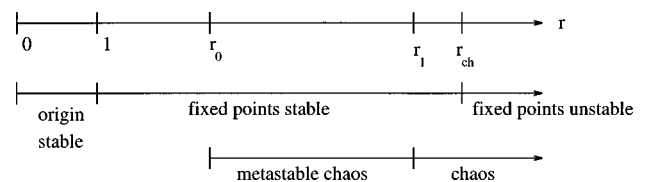

FIG. 2. Regimes of dynamical behavior of the Lorenz equations as a function of the pump parameter r. The threshold for chaos is r_{ch} and metastable behavior is observed for r between the two values r_0, r_1. The fixed points are stable for $1 < r < r_{ch}$.
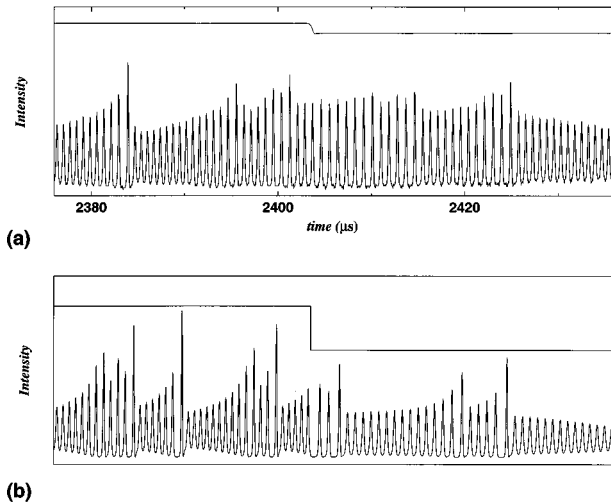
(a)

(b)

FIG. 3. (a) The ring laser intensity (arbitrary units) and pump laser power output. The step in pump level is from slightly above chaos threshold to slightly below (6.4 to 6.0 W). The chaotic pulsations continue for about 20 μs after the switch but with slightly longer period of pulsation, before finally decaying. (b) Calculated intensity for the Lorenz equations with pump parameter switch. Intensity corresponds to the square of Lorenz variable x. $\sigma = 2$, $b = 0.25$, $r = 15.0$ to 10.6. The qualitative behavior compares very well with the experiment, including the slightly longer pulsation period after the switch.

the pump is reduced from above the chaos threshold, r_{ch}, to below the "metastable threshold," r_1.

III. QUALITATIVE BEHAVIOR

Figure 3(a) shows the form of laser intensity with time (lower trace) together with the switch in pump power (upper trace) and Fig. 3(b) is the intensity determined from a numerical integration of the Lorenz equations (see figure caption for parameters) with the associated switch in pump parameter shown as well. In Fig. 3(a), the pump power is switched from one level for which chaos persists indefinitely to slightly below where metastable behavior is observed. Before the switch, chaotic intensity pulsations are present which are "Lorenz-like;" i.e., qualitatively similar to the pulsations from the Lorenz equations shown in Fig. 3(b). After the switch, the pulsations continue to be chaotic and Lorenz-like for a number of pulses until finally switching to a series of pulses where the amplitude is decaying. This behavior is qualitatively the same as that found from the equations and is referred to as "metastable chaos," which was reported in [7]. After switching down below the threshold for chaos, the chaotic dynamics is metastable, in that it continues only for a time before switching to stable behavior. In the equations, the pulsing after the metastable behavior has ceased eventually decays to steady state. In the laser, the pulse amplitudes decay to a fixed level of pulsing [5]. Despite this difference, the overall qualitative behavior of the system and the equations is extremely good. Also reproduced in the numerical integration is the slight increase in the laser pulsation period after the switch.

The change in pulsing period after the switch indicates that when the pump is below chaos threshold, the metastable
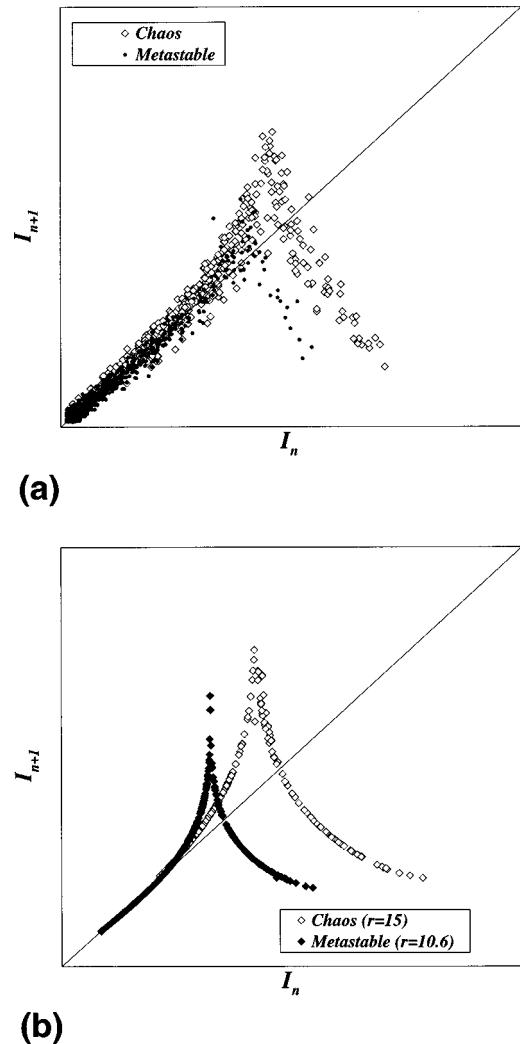

(a)

(b)

FIG. 4. The intensity return maps determined from the time traces shown in Fig. 3 for the experiment (a) and the numerical integration (b). Points marked with open symbols correspond to pairs of pulses occurring before the switch in pump power; solid symbols correspond to pairs of pulses occurring after the switch. A distinct change in the position and form of the "cusp" shape distribution of points is evident after the pump switch, both in the experiment and the numerical analysis.

chaotic attractor is different from the fully chaotic attractor when the pump is above chaos threshold. This is clearly illustrated in Fig. 4 where the return maps [4] for the experimental and numerical time series are plotted, respectively. The return map consists of plotting the value of intensity of one pulsation peak versus the previous peak value. A "cusp" shape distribution is characteristic of the Lorenz equations for a particular value of the pump parameter. If the pump parameter is changed, then the return map will change, reflecting a change in the attractor. As can be seen in both (a) and (b) in Fig. 4, there are two such cusp shapes for each figure where the open and solid symbols correspond to peaks before and after the pump switch, respectively. This demonstrates that the form of the attractor is different before and after the pump switch, as expected. The metastable nature of the dynamics is also evident in the solid-symbol cusp in that the lower end of the left "limb" of the cusp is below the 45° line used to follow the evolution of points in the return
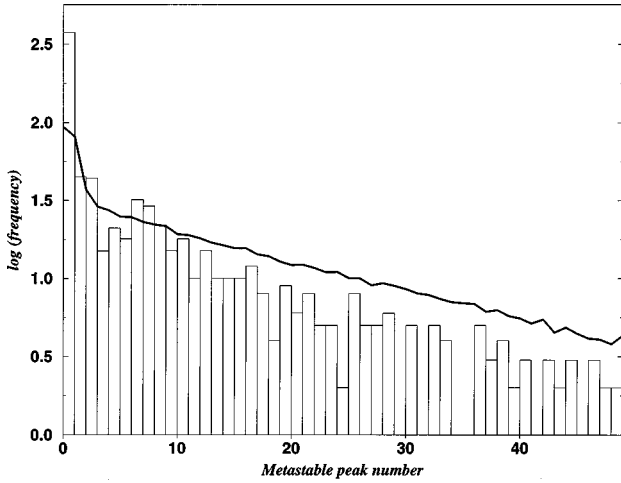
FIG. 5. Frequency distribution of metastable pulsing train lengths. The solid line represents results from $n=10^5$ numerical integrations of the Lorenz equations for the parameters $\sigma=2$, $b=0.25$, $r=15.0$ to 10.6. The histogram is the result of $n=859$ experimental samples of metastable pulsing where the pump power is switched between 6.2 and 5.8 W. The calculated distribution is normalized to the number of samples in the experimental distribution.

map [13]. Once a point maps to this region of the cusp, subsequent mappings result in a monotonic, nearly exponential decay of the peak heights onto the fixed point. When the decay from the metastable state is slow, as in our results, the points lie only slightly below the 45° line, but careful inspection of Figs. 4(a) and 4(b) confirms that the points do lie below the line. The open-symbol points, which represent the chaotic case, all lie on a cusp above this line so that no decay occurs. Qualitative agreement between the theory and experiment is once again good.

IV. STATISTICAL BEHAVIOR

The length of the metastable period depends sensitively on the initial conditions, so if the experiment is repeated many times a statistical distribution can be plotted, giving the relative frequency of occurrence of metastable period lengths, expressed as numbers of pulses. The distribution for the Lorenz equations has been shown to be exponential [7] although this demonstration was made using an empirical determination of the maximum peaks from a scalar function approximation to the map. In Fig. 5 the logarithm of the frequency distribution is shown for both the experiment (histogram) and using full numerical integration (solid line). In the experiment, the pump was repeatedly switched between two values for chaos and metastable behavior and for each switch, the number of metastable pulses before decaying to periodic pulsing was recorded. The numerical integration was performed similarly so as to closely follow the experiment. The numerical calculations show much less variation due to the large number of samples taken (10^5). In the experiment, the number of samples was limited by the data acquisition memory size and constancy of experimental parameters over the time of sampling to about 1 ms. Although the control over system parameters for most purposes was sufficient, the extra sensitivity of metastable behavior to

small changes in parameters required rapid data sampling to minimize the drift of conditions. Nevertheless, the experimental histogram shows a reasonable linearity over the log-linear scale, with the exception of metastable periods of length zero, one, or two pulses. Both the experiment and the numerical integration show a deviation from a pure exponential distribution for these low numbers of metastable pulses. The mechanism for this will be discussed in Sec. V. There are also no counts recorded for some of the histogram bins, which is simply due to the small number of samples in the whole distribution.

If the first few bins which deviate strongly from a purely exponential distribution are omitted, the slope of the remaining plot is then the mean of the distribution. Alternatively, when there are insufficient samples to generate a representative histogram, the mean of the frequency distribution may be determined by taking the simple mean of the sample of metastable pulse series, excluding series with less than three metastable pulses. The experimental distribution was also limited by the largest number of pulses that could occur before the pump is switched back up to reestablish chaos. Therefore the mean μ of the effective exponential distribution, $P(x)=(1/\mu)e^{-x/\mu}$, is determined from the measured mean μ_{meas} via

$$\mu_{\text{meas}}=\frac{\int_3^{N_{\max}}xP(x)dx}{\int_3^{N_{\max}}P(x)dx},\qquad(4.1)$$

where $N_{\max}$ is the maximum number of metastable pulses that could occur in any one series before the pump was switched back to the value for chaos. For each value of μ_{meas} obtained, the corresponding value of μ was obtained by numerical solution of $[\mu_{\text{meas}}(\mu)-\langle N\rangle]=0$, where $\langle N\rangle$ is the experimentally obtained average number of metastable pulses, and $\mu_{\text{meas}}(\mu)$ is the functional dependence of the measured mean on the effective mean, according to the above equation.

As the pump parameter at which metastable chaos is observed is increased toward the value represented by r_1 in Fig. 2, the expectation is that the mean number of metastable pulses should tend rapidly to infinity, since above this value the chaotic attractor is stable and trajectories in phase space should remain chaotic. This was clearly observed in the experiment. An average metastable pulsing length could be observed on an oscilloscope display that lengthened as the pumping was increased to the value for full chaotic behavior. Figure 6 shows the results of measurements quantifying this behavior. The average metastable pulsing length (in terms of the number of pulses) is plotted versus the difference between the pump parameter and the pump value corresponding to r_1, on logarithmic scales. This demonstrates an exponential increase in the average metastable length as the critical pump value is approached. The slope of the line of best fit is referred to as the critical exponent, after [10], and has also been experimentally measured elsewhere [11,12]. The error bars are relatively large due to the requirement for rapid sampling over a short enough time to minimize the drift of conditions.

Figure 7 shows a comparison of the experimental variation measured together with that of the numerically inte-
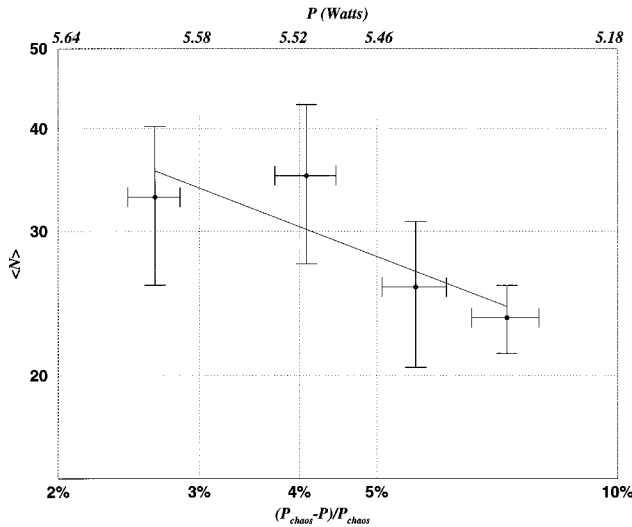
FIG. 6. Average metastable pulsing length (in terms of number of pulses) plotted versus the difference between the pump parameter and the pump value corresponding to r_1 (normalized to r_1) with logarithmic scales. Pump powers used are from 5.4 to 5.7 W. Chaos is first observed at 5.75 W. Number of samples of metastable transients vary from 86 at high pump powers to 430 at low pump powers.

grated Lorenz equations using the parameters used in this work and also for the functional parametrization used in [7]. We also numerically verify the values of [7] using the same parameters, $\sigma = 10$, $b = 8/3$. The critical exponents for each curve are listed in Table I. The observed qualitative behavior is clearly represented in the experiment and is consistent with expectations and with the behavior of the Lorenz equations.

As can be seen from the slope and position of the curves in Fig. 7 and Table I there is a wide variation and the values of the exponent appear to be dependent upon the system parameters. Also the value calculated for $\sigma = 2$, $b = 1/4$ deviates from exponential at r values far from the metastable threshold value. The critical exponent listed in Table I for these parameters was calculated using the linear portion of the curve. Although there does not appear to be a universal exponent for the Lorenz system, and hence presumably for the experiment, the general behavior upon approach to the metastable threshold is common to all.

V. VISUALIZATION OF THE BASINS OF ATTRACTION

The Lorenz equations are time derivatives to first order and contain no explicit time dependence. Thus the dynamics is dependent solely on the parameters, σ, b, r and the initial conditions, x_0, y_0, z_0. Referring to Fig. 2, if the pump parameter is chosen in the region $r_1 < r < r_{ch}$ it follows that where the initial conditions are chosen in phase space will determine their subsequent behavior. As already discussed, if the conditions are chosen in the basin of attraction of the chaotic attractor, the system will remain chaotic. Similarly, the system will go to one of the fixed points if the initial conditions are chosen as part of the fixed point's basin of attraction. In the experiment, the initial conditions are limited to points on the attractor of the system when evolving chaotically. When
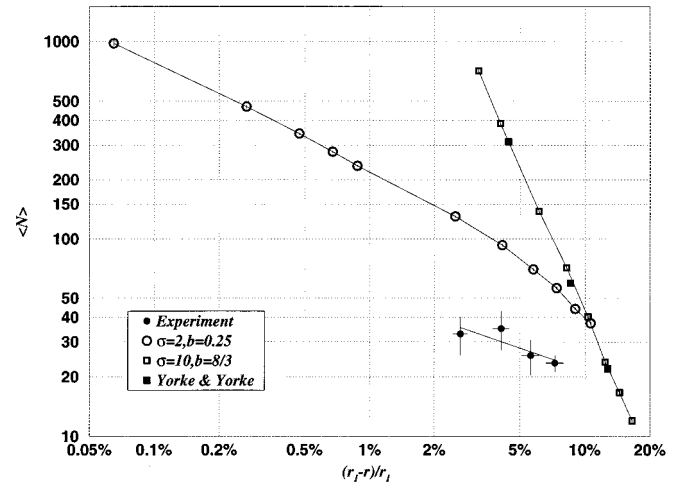

FIG. 7. Determination and comparison of critical exponents for the experiment and the Lorenz equations. The parameters of Yorke and Yorke [7] are $\sigma = 10$, $b = 8/3$, $r = 22$ to 24, $r_{ch} \approx 24.74$, $r_1 \approx 24.06$. The parameters used in this work are $\sigma = 2$, $b = 1/4$, $r = 11.0$ to 12.3, $r_{ch} = 14$, $r_1 \approx 12.308$.

the pump is suddenly switched to a metastable regime value, the state of the system before the switch represents the initial conditions chosen. However, in the numerical integrations, any point in phase space may be arbitrarily chosen, regardless of whether or not it represents the state of the real experimental system at any time. Thus the whole phase space may be mapped and the various basins of attraction readily identified.

Figure 8 shows such a map for a value of the pump parameter in the metastable regime. Each point in three dimensions represents an initial condition. The surface shown is the boundary defined by whether a chosen initial condition, when evolved, either immediately decays to one of the fixed points, or whether it first evolves in a metastable chaotic fashion. The former are points inside the surface and the latter are all other points outside. The evolution of a single initial condition, which is outside the surface, is also shown (white) from which the chaotic nature of the metastable trajectory can be seen. The map shows a remarkable structure that is otherwise hidden due to the choice of initial conditions. There are two tubelike extensions of the surface which cross each other in the manner of a simple overhand knot. The tubes pass through the plane of the metastable attractor at the positions of the fixed points. This is consistent with the fact that the fixed points are stable and any trajectories that are close to these spiral inward. However, it can be seen that this immediate attraction to the fixed points is not limited to the planes of the attractor but extends outward, defined by the interior volume of the tubes. The tubes continue away from the origin along the x axis, in both directions, forming a corkscrew (not shown).

TABLE I. Critical exponents determined from the lines of best fit (Fig. 7).

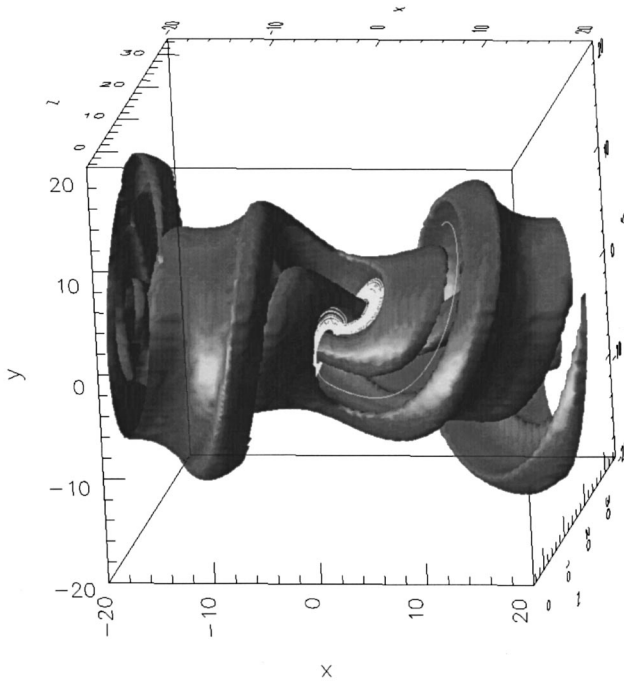|	
Experiment	0.376
$\sigma = 2$, $b = 1/4$	0.567
$\sigma = 10$, $b = 8/3$	2.50

FIG. 8. Three-dimensional phase space map of the basin of attraction for metastable chaos. x, y, z correspond to the variables of the Lorenz equations. Parameters are $\sigma = 2$, $b = 1/4$, $r = 10.6$, $r_{ch} = 14$. The white trajectory is the metastable evolution of a single initial condition chosen very close to the defined surface. See text for description.

The surface shown is, in fact, only part of the complete surface which has been removed for clarity. The nature of the removed portion is presented in Fig. 9, which is a planar slice through the phase space of Fig. 8 along the y-z plane at $x = 0$. In Fig. 9, the points are shaded according to whether they immediately evolve to either fixed point (black) or in-
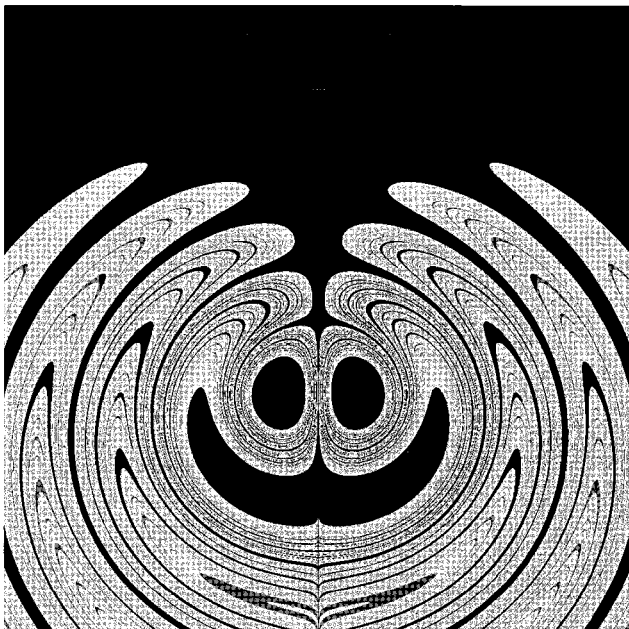

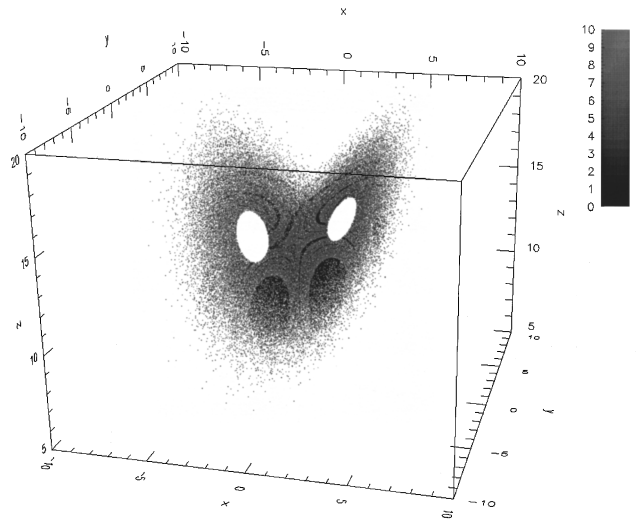FIG. 9. y-z slice at $x = 0$ through phase space of the map shown in Fig. 8.

FIG. 10. Three-dimensional presentation of the initial conditions chosen to observe metastable behavior. The initial conditions are part of the attractor for $\sigma = 2$, $b = 1/4$, $r = 15 > r_{ch} = 14$. Points are shaded according to the number of metastable pulses executed before decaying to the fixed points when r is switched to $r = 10.6$. Black points correspond to initial conditions which decay directly to the fixed points.

stead execute metastable pulsing (lighter shades of gray for longer metastable pulsing). The two black circular regions and the black ''mouth-shaped'' region correspond to the cross sections in the y-z plane of the two tubes and the outer surface in Fig. 8. It can be seen from Fig. 9 that the whole object of Fig. 8 is encased in a series of black ''shells'' and, in fact, much of the phase space at high values of z is also black, corresponding to initial conditions which directly evolve to the fixed points. Furthermore, there are black regions that are interposed between metastable regions in a fractal-like manner. Although not clear from these figures, the surface from which the tubes extend pinches into a sheet which folds in between the metastable chaotic attractor, giving rise to the observed interposition of black and metastable regions so that there are also points in the plane of the attractor which decay immediately to the fixed point instead of first executing a metastable chaotic orbit.

It is not the intention of this work to fully describe the structure unveiled by the phase space map shown. Instead, at present, we merely obtain an intuitive understanding of the metastable dynamics observed using the above picture. In the experiment, as already mentioned, the initial conditions are not arbitrary points in the described phase space but rather correspond to points on the chaotic attractor. When the system is chaotic all the points lie on the attractor, therefore when the pump is switched below the chaos threshold the initial condition must lie on the attractor. This is depicted in Fig. 10 where each initial condition was obtained from a numerical integration of the Lorenz equations in the chaotic regime. Each initial condition is shaded depending upon whether it immediately decays to the fixed point, or first evolves chaotically. In this case, the points which evolve directly to the fixed points are black. Clear regions are points that are never visited by the chaotic trajectory and hence never chosen as initial conditions. Figure 10 is effectively a

subset of the phase space shown in Fig. 8 where the points are selected by the chaotic orbit for when the system is evolving at a pump parameter value above r_{ch}.

All points in Fig. 10 lie on a fully chaotic attractor that is around the unstable fixed points with z coordinate, $r-1$. This attractor is in a different position in phase space to that of the metastable attractor shown in white in Fig. 8 for which r is less than r_1. The chaotic attractor is higher along the z axis than the metastable attractor shown in the map. Evident are two circular white regions where no points are chosen. Since the chaotic attractor never visits these regions of phase space, these are never initial conditions for metastable chaos. Also present are two black circular areas below the aforementioned white regions. These are initial conditions which immediately decay to the fixed points. Comparing this area with the phase space map of Fig. 8, it can be noted that this is where the chaotic attractor for $r>r_{ch}$ intersects the tubes of the surface shown in Fig. 8 wherein $r<r_1$. Since the chaotic attractor intersects the surface, if r is switched down when the chaotic trajectory is inside the surface, the initial conditions are then those inside the surface which, by definition, means the trajectory subsequently spirals to the fixed points.

By comparing the relative area between the black and all other shaded points in Fig. 10, it can be seen that there is a larger proportion of initial conditions chosen that evolve immediately to the fixed points. This qualitatively explains why there is a deviation from exponential in the histogram in Fig. 5. Since there is some kind of structure in phase space as depicted by Fig. 8, the way in which the initial conditions are chosen will determine the form of the distribution to an extent. In the extreme, if all initial conditions are chosen when the chaotic trajectory is in the dark regions, then there will be no metastable transients. This has implications for the design of algorithms to control chaotic behavior as rapid targeting of the steady state could be achieved by careful choice of the switching time. The way in which the points are chosen in the experiment corresponds to points on a chaotic orbit such as in Fig. 10 and hence there is a larger sampling of the initial conditions inside the surface of Fig. 8. Further inspection of Fig. 10 shows there is structure in the form of black lines and curves. These correspond to the previously described fractal-like interposing of the metastable and fixed point basins of attraction resulting from the pinching and folding of the surface in Fig. 8 throughout the metastable attractor.

VI. CONCLUSION

Our experiments have shown that when the pump power in the ammonia laser is reduced below the threshold for long-term chaos the transition to the new asymptotic state can be via a period of metastable chaos exactly as predicted for the Lorenz equations. The form of the unstable attractor is similar to that of the stable Lorenz attractor and the distribution of lengths of metastable chaos observed is exponential except that there is an excess of short lengths. This can be related to the overlap between the basin of attraction of the stable fixed point and the set of available initial conditions which is the chaotic attractor which was stable before the switch.

[1] C. O. Weiss and J. Brock, Phys. Rev. Lett. **57**, 2804 (1986).

[2] H. Haken, Phys. Lett. **53A**, 77 (1975).

[3] E. N. Lorenz, J. Atmos. Sci. **20**, 130 (1963).

[4] M. Y. Li, Tin Win, C. O. Weiss, and N. R. Heckenberg, Opt. Commun. **80**, 119 (1990).

[5] Tin Win, M. Y. Li, J. T. Malos, N. R. Heckenberg, and C. O. Weiss, Opt. Commun. **103**, 479 (1993).

[6] M. Y. Li and N. R. Heckenberg, Opt. Commun. **108**, 104 (1994).

[7] J. A. Yorke and E. D. Yorke, J. Stat. Phys. **21**, 263 (1979).

[8] C. Grebogi, E. Ott, and J. A. Yorke, Physica D **7**, 181 (1983).

[9] C. Z. Ning and H. Haken, Phys. Rev. A **41**, 6577 (1990).

[10] C. Grebogi, E. Ott, F. Romeiras, and J. A. Yorke, Phys. Rev. A **36**, 5365 (1987).

[11] M. Finardi, L. Flepp, J. Parisi, R. Holzner, R. Badii, and E. Brun, Phys. Rev. Lett. **68**, 2989 (1992).

[12] I. M. Jánosi, L. Flepp, and T. Tél, Phys. Rev. Lett. **73**, 529 (1994).

[13] C. Sparrow, *The Lorenz Equations: Bifurcations, Chaos, and Strange Attractors* (Springer-Verlag, New York, 1982).